JACOBS PUBLISHERS

OPEN ACCESS

Jacobs Journal of Radiation Oncology

Case Report

# Morbidity Associated with False-Positive Findings in Post-Treatment Positron Emission Tomography/Computed Tomography in Chemoradiation Treated Head and Neck Cancer Patients

Sun K. Yi[1*], M.D., Sarah Kratz[2], M.D., TJ Gernon[3], M.D., Audrey Erman[3], M.D., Rihan Khan[4], M.D., Ryan Avery[4], M.D., Fatima Aly[5], M.D., Phillip H. Kuo[4], M.D., Ph.D., Michael K. Cheung[1], M.D., Georgi Georgiev[6], M.S.

[1]*Department of Radiation Oncology, Arizona Cancer Center, University of Arizona Medical Center, Tucson, AZ, USA*

[2]*Department of Hematology/Oncology, Arizona Cancer Center, University of Arizona Medical Center, Tucson, AZ, USA*

[3]*Department of Surgery, Division of Head and Neck Surgery, Arizona Cancer Center, University of Arizona Medical Center, Tucson, AZ, USA*

[4]*Department of Medical Imaging, Arizona Cancer Center, University of Arizona Medical Center, Tucson, AZ, USA*

[5]*Department of Pathology, University of Arizona Medical Center, Tucson, AZ, USA*

[6]*Department of Radiation Oncology, Division of Medical Physics, Arizona Cancer Center, University of Arizona Medical Center, Tucson, AZ, USA*

**Corresponding author: Dr. Sun K. Yi, M.D., 1501 N Campbell Ave, PO Box 245081,Tucson, AZ 85724 , USA, Tel: (520) 694-7236; E-mail:Sunkyi@email.arizona.edu*

*Received:* 08-04-2014

*Accepted:* 12-08-2014

*Published:* 12-11-2014



## Abstract

Positron emission tomography/computed tomography (PET/CT) for chemoradiation treated Head and Neck (HN) cancer is often utilized for post-treatment surveillance. Early detection of persistent or recurrent disease may allow for surgical salvage, however false positive or ambiguous findings on initial PET/CT surveillance may lead to premature invasive intervention and associated morbidity. We present a case of a 58 year old male treated definitively with chemoradiation for locally advanced HN squamous cell carcinoma (SCC) who presented with ambiguous initial 90 day post treatment PET/CT, leading to biopsy and subsequent progressive radionecrosis and superinfection.

**Keywords:** PET/CT; Radiation Therapy; Head and Neck Cancer; Optimal Timing; False Positives

## Introduction

Positron Emission Tomography/Computed Tomography (PET/CT) is a powerful tool in Head and Neck (HN) cancer surveillance [1], however optimal timing of PET/CT acquisition after chemoradiation remains unclear. The early detection of salvageable disease must be carefully balanced against those findings associated with resolution of treatment related inflammation that occur over many weeks following therapy [2]. False positive findings on PET/CT have been described and often lead to heightened provider/patient anxiety, premature invasive intervention and associated morbidities. We present a patient treated with definitive chemoradiation for locally advanced HN cancer with ambiguous initial post-treatment PET/CT findings, leading to biopsy, progressive radionecrosis and superinfection.

## Case Presentation

Our patient is a 58 year-old Caucasian male who presented

with progressive oropharyngeal symptoms including dysarthria, dysphagia, odynophagia, right-sided otalgia, tongue dysesthesias and swelling. He was found to have a large friable and exophytic right base of tongue (BOT) mass crossing midline, extending onto the right aryepiglottic (AE) and pharyngoepiglottic folds, tethering into the right glossotonsillar sulcus, and effacing both the ipsilateral vallecula and piriform sinus. The patient had limited tongue mobility and no palpable cervical lymphadenopathy. The mass was biopsied and found consistent with poorly differentiated squamous cell carcinoma (SCC). Staging PET/CT scan (Figure 1a) showed a large right BOT mass with extension inferiorly to the level of the AE folds, demonstrating pathological erosion of the hyoid bone. It had a standardized uptake value (SUV) of 18.2 and measured 6.7x4.7x4.4cm in the antero-posterior, tranverse, and cranial-caudal dimensions, respectively. Cervical lymph nodes were not enlarged by CT criteria but several did demonstrate increased 2-[$^{18}$F]-fluoro-2-deoxy-D-glucose (FDG) uptake. The patient was staged T4aN2cM0 by AJCC criteria.

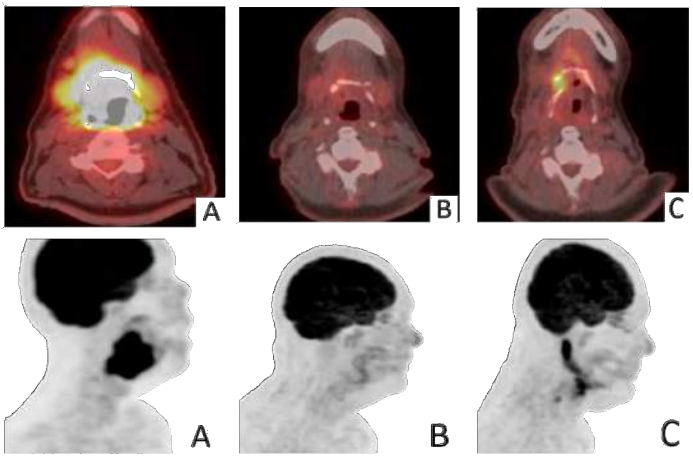


**Figure 1** (a). Representative axial and right anterior oblique images of pre-treatment PET/CT at the level of the hyoid, demonstrating a large hypermetabolic right BOT SCC with hyoid necrosis; (b) 90 day post-treatment PET/CT images with focus of ambigous uptake near the region of hyoid necrosis; (c) 225 day post-treatment PET/CT images with hypermetabolic activity of the posterior digastric muscle representing retrograde polymicrobial infection.

Treatment options were presented to the patient and he opted for definitive chemoradiation. He was treated with concurrent cisplatin based therapy. Over the course of treatment, the patient suffered expected acute toxicities including grade 2 mucositis, dysgeusia, xerostomia, skin erythema, odynophagia, weight loss, and transient grade 1 anemia. He successfully completed all planned treatment with minimal interruption and no cisplatin dose reduction. He demonstrated clear clinical and radiographic response by finger palpation and daily megavoltage CT. One month following completion of therapy, the patient had resolution of all toxicities and was found with a complete clinical disease response.

At the time of initial PET/CT scan, taken 90 days post-treatment (Figure 1b), the patient reported intermittent right otalgia, but otherwise was feeling well. PET/CT revealed a dramatically reduced right oropharyngeal mass demonstrating an SUV of 4.3 compared with 18.2 prior to the start of treatment. Pathologic erosive changes of the hyoid bone were again seen with mild residual hypermetabolic activity and interval development of reparative changes. Given the ambiguous SUV uptake, the patient's case was discussed at our HN tumor conference. It was agreed that the patient would require further work-up. Therefore, the patient was taken to the operating room for direct laryngoscopy and biopsies. Intraoperatively, necrotic tissue was located in the posterior right glossotonsillar sulcus. Biopsies were taken and an exposed artery was clipped. Pathology revealed scattered ghost and pyknotic cells consistent with tumor necrosis, but there was no evidence of viable malignancy (Figure 2).

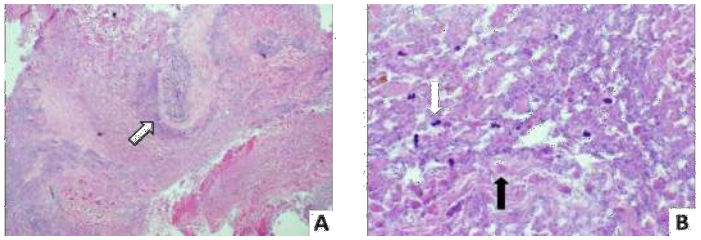


**Figure 2**. Histopathology – Hematoxylin and Eosin (H&E) stained specimens (a) 4x magnification view exhibits marked areas of necrosis (hollow arrow) (b) 40x magnification view demonstrates ghost cells (solid black arrow), scattered degenerate cells with pyknotic nuclei (white arrow), and no viable malignant cells.

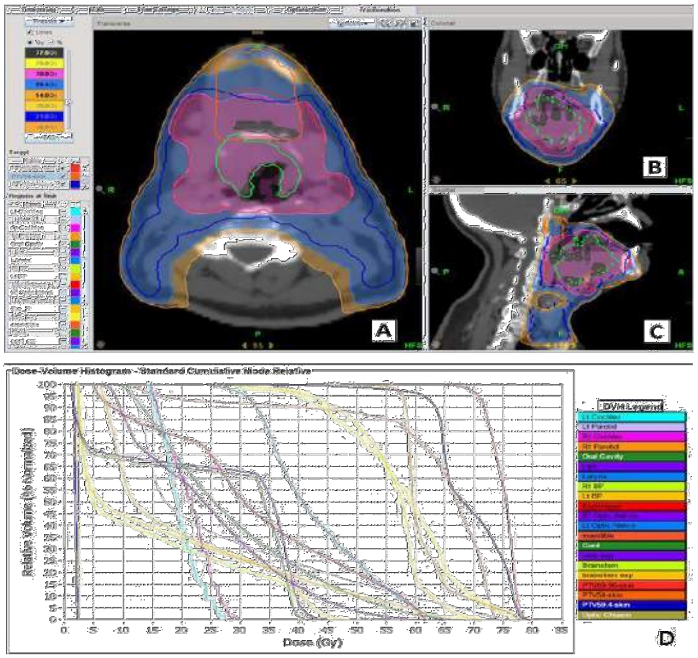


**Figure 3** (a). Representative axial slice of isodose distributions overlying respective planned target volumes (PTVs) at the level of the hyoid bone; (b) Representative coronal slice of isodose distributions

overlying respective PTVs at the corresponding area of hyoid necrosis seen in Figure 2a; (c) Representative sagital slice of isodose distributions overlying respective PTVs at the corresponding area of hyoid necrosis seen in figure 2a; (d) Dose Volume Histogram (DVH).

Immediately post-biopsy, the patient developed rapid regression of his near-complete resolution in disease-related speech and swallowing dysfunction. One month later, he developed an edematous right BOT and atrophy of his anterior right tongue. Tongue motion was limited and speech was indiscernible. The patient was started on pentoxyfilene, vitamin E, and methylprednisolone for presumed radiation necrosis. He was also referred to speech and swallow therapy. The patient was followed every 1-2 months with persistent speech and swallowing impairment. Repeat endoscopic examination showed persistent right BOT edema with necrosis in the glossotonsillar sulcus. PET/CT at 225 days post-therapy (Figure 1c) revealed a new linear area of abnormal FDG avidity extending from the right mastoid to the hyoid bone (SUV 11.6). Erosive changes of the hyoid were again visualized. MRI was taken for further delineation and revealed post-therapy changes in the right BOT without definitive evidence of abnormal enhancement or disease recurrence. Edema and mild peripheral enhancement were seen within the posterior right digastric muscle corresponding to the area of increased FDG uptake. The patient was initiated on an 8-week course of broad spectrum antibiotics for presumed polymicrobial infection.

## Materials and Methods

### PET/CT skull to mid-thigh:

Prior to imaging, fingerstick blood glucose level was measured. Intravenous (IV) injection of $^{18}$F-FDG was performed at least 1 hour prior to image acquisition. CT was performed at low dose without IV contrast, except for the initial scan. Scans extended from the skull vertex to the upper thighs. For the initial PET/CT, standard iterative reconstruction was performed. The subsequent PET/CT scans were reconstructed using a time of flight algorithm. Images were reformatted in all three planes and maximum intensity projections were constructed. Maximal SUV values were reported by the interpreting nuclear medicine physician.

During initial PET/CT, patient blood glucose measured 90 mg/dl. The patient received 15.9 millicuries (mCi) of $^{18}$F-FDG prior to imaging. At 90-day PET/CT, patient blood glucose was 107 mg/dl and he received 7.5 mCi of $^{18}$F-FDG. At 225-day PET/CT, patient blood glucose was 112 mg/dl and he received 7.5 mCi of 18F-FDG.

### Radiotherapy

Simulation was performed with GE Lightspeed series PET/CT scanner (Little Chalfont, UK). HN aquaplast mask and bite block were utilized for immobilization and intraoral stabilization. CT images were acquired from skull vertex to mid-thorax after 100cc of isoview contrast was administered. PET imaging was taken after administration of 15.9 mCi of $^{18}$F-FDG. All images were then imported into Philips Pinnacle v. 9.0 treatment planning software (Andover, MA) for physician contouring.

Gross Tumor Volume (GTV) was delineated on IV-enhanced, FDG avid tumor. Five millimeter (mm) uniform margin was applied to GTV utilizing Pinnacle auto-expansion tool to create clinical target volume (CTV) 69.96 with editing to respect normal anatomic boundaries. High risk nodal volume CTV 59.4 was created utilizing the RTOG endorsed HN contouring atlas [3] and included bilateral levels IB through III and the superior portion of right level IV. Elective nodal volume CTV 54 included the inferior aspect of right level IV, left level IV, and bilateral retropharyngeal regions. All CTVs were then expanded uniformly by 5mm to create respective planned target volumes (PTVs). Normal tissues were contoured including: optic nerves and chiasm, brainstem with 3mm expansion, bilateral cochleas, spinal cord with 5mm expansion, bilateral parotid glands, lips, oral cavity, mandible, superior constrictor muscles, larynx, esophagus, and bilateral brachial plexi.

Inverse planning with intensity modulated radiation therapy (IMRT) was utilized on Tomotherapy v. 5.0 planning station (Sunnyvale, CA). Simultaneous integrated boost was used to treat PTV 69.96 to 69.96 Gy in 2.12 Gy, PTV 59.4 to 59.4 Gy in 1.8 Gy, and PTV 54 to 54 Gy in 1.64 Gy daily fractions, respectively. Normal tissues were constrained according to well accepted guidelines [4]. Ninety seven percent, 97% and 99% of PTV 69.96, PTV 59.4 and PTV 54 were covered by their prescription isodose lines, respectively. Thirty five cc of PTV 69.96 received 77 Gy (110% of the prescription) and 21.6 cc of the GTV received 77 Gy. A point maximum dose of 80.9 Gy (116% of the prescription) was delivered. All normal tissue constraints were met except for the left parotid gland, mandible, and bilateral brachial plexi given substantial overlap with PTV 69.96. Representative axial, coronal and sagittal isodose distributions, and the dose-volume histogram (DVH) are shown in Figures 3a-d.

Patient specific quality assurance was performed by the physics division. The plan passed institutional parameters of less than 3% difference or less than 3mm geographic discrepancy between planned and delivered dose. The patient was treated once daily (Monday through Friday) for 33 total fractions with daily megavoltage CT image guidance on the Tomotherapy linear accelerator.

### Chemotherapy

The patient received 3 cycles of cisplatin chemotherapy ev-

ery 21 days beginning with the start of radiotherapy. He was pre-medicated with 0.25mg of IV palonosetron and 10mg of IV dexamethasone in 750ml of 0.9% normal saline. For each cycle, 100 mg/m$^2$ of cisplatin was infused in 1000ml of 0.9% normal saline with 20 mEq of KCl and 2g of magnesium sulfate over 2 hours. Five hundred ml of 0.9% normal saline was given for post-hydration. A three day course of aprepitant was given after each cycle of chemotherapy. The patient was followed with weekly complete blood count and comprehensive metabolic panel.

## Discussion

Definitive chemoradiation is considered standard of care for patients diagnosed with locally advanced HNSCC [5]. Despite aggressive management, locoregional failures remain a substantial problem [6], but are salvageable with surgical intervention [7]. Early detection of persistent or recurrent disease is therefore paramount to optimal patient outcome.

Post-treatment evaluation for HN cancer has historically been rendered by history and physical examination. There is no consensus among NCCN members for recommending imaging surveillance, though it is commonly practiced [8]. PET/CT offers improved accuracy over conventional techniques and is frequently used for HN cancer surveillance [9]; however, its role remains controversial as there is significant heterogeneity among inter-institutional scanning protocols and limited prospective data on its clinical impact to patient and oncologic outcomes. In a recent review by Patel et. al.[10], four prospective trials in HN cancer PET or PET/CT surveillance were analyzed and was reported that positive predictive values (PPV) ranged from 50-90% and specificities between 85-95%, suggesting that false positives remain a significant challenge to treating physicians. Another meta-analysis reviewing post-treatment PET/CT reported weighted means of 52-59% and 88% for PPV and specificity, respectively [11].

Invasive procedures including restaging biopsy of ambiguous FDG avid areas within recently irradiated fields may introduce unnecessary morbidity to patients and exacerbate chronic late radiation toxicity. These adverse events have been described in other disease sites treated by chemoradiation [12] and intervention is generally recommended against unless clear disease progression is found. Total radiation dose, inherent patient related factors, and invasive procedures in irradiated fields have all been implicated in increasing the risk for developing radiation necrosis [13]. Deep neck infections are clinically challenging and often polymicrobial complications with occasionally fatal outcomes, and have been attributed to iatrogenic etiologies as well [14].

Our patient developed a region of necrosis near the epicenter of his treated right BOT malignancy. This area received the full dose of 69.96 Gy with "hot spots" approaching 77 Gy abutting the area of mucosal ulceration. A point maximum dose of 80.9 Gy (116% of the prescription) was found within the anteromedial aspect of PTV 69.96, which was near the focus of residual uptake found on the 90 day post-treatment PET/CT. It remained unclear whether this area of necrosis and residual hypermetabolic activity on PET/CT represented persistent malignancy versus treatment related inflammation, though no obvious gross tumor was seen. Biopsy confirmation was performed after agreement was reached by our institutional tumor board and pathology revealed extensive necrosis without evidence of viable malignancy.

The patient subsequently developed rapid loss in oropharyngeal function which was recovered following his complete response to therapy. A multimicrobial infection was likely introduced into the nidus of smoldering radionecrosis at the posterior right glossotonsillar sulcus.

Endoscopic vascular clipping of an exposed artery likely contributed to local hypoxia and progression of the radionecrosis [15]. Infection then tracked posteriorly along the posterior belly of the right digastric muscle at its insertion onto the hyoid bone to the mastoid tip (Figure 1c).

Though it has been clearly demonstrated that PET/CT taken after definitive management is superior for detection of persistent or recurrent malignancy over more conventional imaging [9,16], the optimal timing of PET/CT acquisition after therapy remains unclear. There is suggestion that PET/CT imaging should be performed between 2-4 months post-therapy for optimized accuracy of disease detection [17-19], although other data suggest delaying scans even further [16]. Our patient was scanned at 3 months post-therapy and may have benefitted from delayed initial PET/CT scanning or short follow-up with 1-2 month interval PET/CT to monitor SUV kinetics.

## Conclusion

The optimal timing of initial PET/CT after definitive chemoradiation therapy for HNSCC remains unclear. We propose that patients without clear evidence of disease progression but with equivocal findings on initial post-therapy PET/CT scan be followed with short interval PET/CT for assessment of SUV kinetics and guidance for the need of additional invasive procedures.

## References

1. Heron DE, Andrade RS, Beriwal S, Smith RP. PET-CT in Radiation Oncology: The Impact on Diagnosis, Treatment Planning, and Assessment of Treatment Response. Am J Clin Oncol. 2008, 31(4): 352-362.

2. Andrade RS, Heron DE, Degirmenci B, Filho PA, Branstetter BF et al. Posttreatment assessment of response using FDG-PET/CT for patients treated with definitive radiation therapy for head and neck cancers. Int J Radiat Oncol. 2006, 65: 1315–1322.

3. Marks LB, Yorke ED, Jackson A, Ten Haken RK, Constine LS et al. Use of Normal Tissue Complication Probability Models in the Clinic. Int J Radiat Oncol Biol Phys. 2010, 76 (3 Suppl): S10–S19.

4. Ang KK, Harris J, Wheeler R, Weber R, Rosenthal DI et al. Human Papillomavirus and Survival of Patients with Oropharyngeal Cancer. N Engl J Med. 2010, 363(1): 24–35.

5. Pignon JP, le Maître A, Maillard E, Bourhis J; MACH-NC Collaborative Group. Meta-analysis of chemotherapy in head and neck cancer (MACH-NC): An update on 93 randomised trials and 17,346 patients. Radiother Oncol. 2009, 92(1): 4–14.

6. Tan HK, Giger R, Auperin A, Bourhis J, Janot F et al. Salvage surgery after concomitant chemoradiation in head and neck squamous cell carcinomas—Stratification for postsalvage survival. Head Neck. 2010, 32(2): 139–147.

7. National Comprehensive Cancer Network. NCCN Clinical Practice Guidelines in Oncology: Head and Neck Cancers. Version 2.2013.

8. Kostakoglu L, Fardanesh R, Posner M, Som P, Rao S et al. Early Detection of Recurrent Disease by FDG-PET/CT Leads to Management Changes in Patients With Squamous Cell Cancer of the Head and Neck. Oncologist. 2013, 18(10):1108-1117.

9. Patel K, Hadar N, Lee J, Siegel BA, Hillner BE et al. The Lack of Evidence for PET or PET/CT Surveillance of Patients with Treated Lymphoma, Colorectal Cancer, and Head and Neck Cancer: A Systematic Review. J Nucl Med. 2013, 54(9): 1518-1527.

10. Gupta T, Master Z, Kannan S, Agarwal JP, Ghsoh-Laskar S et al. Diagnostic performance of post-treatment FDG PET or FDG PET/CT imaging in head and neck cancer: a systematic review and meta-analysis. Eu. J Nucl Med Mol Imaging. 2011, 38(11): 2083–2095.

11. Glynne-Jones R, Northover JMA, Cervantes A, On behalf of the ESMO Guidelines Working Group. Anal cancer: ESMO Clinical Practice Guidelines for diagnosis, treatment and follow-up. Ann Oncol. 2010, 21(5): v87–v92.

12. Beumer J, Silverman S, Benak SB. Hard and soft tissue necroses following radiation therapy for oral cancer. J Prosthet Dent. 1972, 27(6): 640–644.

13. Huang TT, Liu TC, Chen PR, Tseng FY, Yeh TH et al. Deep neck infection: analysis of 185 cases. Head Neck. 2004, 26(10): 854–860.

14. Wong CS, Van der Kogel AJ. Mechanisms of radiation injury to the central nervous system: implications for neuroprotection. Mol Interv. 2004, 4(5): 273-284.

15. Kubota K, Yokoyama J, Yamaguchi K, Ono S, Qureshy A et al. FDG-PET delayed imaging for the detection of head and neck cancer recurrence after radio-chemotherapy: comparison with MRI/CT. Eur J Nucl Med Mol Imaging. 2004, 31(4): 590–595.

16. Greven KM, Williams DW 3rd, McGuirt WF Sr, Harkness BA, D'Agostino RB Jr et al. Serial positron emission tomography scans following radiation therapy of patients with head and neck cancer. Head Neck. 2001, 23(11): 942–946.

17. Isles MG, McConkey C, Mehanna HM. A systematic review and meta-analysis of the role of positron emission tomography in the follow up of head and neck squamous cell carcinoma following radiotherapy or chemoradiotherapy. Clin Otolaryngol. 2008, 33(3): 210–222.

18. Lowe VJ, Boyd JH, Dunphy FR, Kim H, Dunleavy T et al. Surveillance for recurrent head and neck cancer using positron emission tomography. J Clin Oncol 2000, 18(3): 651–651.